Applied Surface Science 396 (2017) 1201–1205

Contents lists available at ScienceDirect

Applied Surface Science

journal homepage: www.elsevier.com/locate/apsusc

Full Length Article

Formation of nanostructures induced by capillary-discharge soft X-ray laser on BaF_2 surfaces

Yongpeng Zhao [a], Huaiyu Cui [a,*], Shuqing Zhang [b], Wenhong Zhang [a], Wei Li [a]

[a] National Key Laboratory of Science and Technology on Tunable Laser, Room 102, Block 2A, No.2 Yikuang Street, Nangang District, Harbin Institute of Technology, Harbin, China
[b] Department of Optical Engineering, School of Astronautics, Block B2, No.2 Yikuang Street, Nangang District, Harbin Institute of Technology, Harbin, China

ARTICLE INFO

Article history:
Received 20 July 2016
Received in revised form 19 October 2016
Accepted 14 November 2016
Available online 17 November 2016

Keywords:
Capillary-discharge X-ray laser
Nanostructures
Toroidal mirror
BaF_2

ABSTRACT

BaF_2 was ablated by a capillary-discharge pumped soft X-ray laser at 46.9 nm focused by a toroidal mirror at a grazing incidence of 83°. The damaged area, induced by both single and multiple laser pulses, was determined to be covered with fringe-like nanostructures with spacings of approximately 400 nm and mastoid nanostructures with diameters of approximately 600 nm. In this study, we analyze the morphology of the detected damage patterns and discuss the damage mechanism. Results indicate that the depth of the nanostructures varies with different pulse numbers and laser power densities.

1. Introduction

X-ray laser is always an attractive research topic because of its high photon energy. Studying the interaction process between X-ray laser and matter is of great importance to fundamental science as well as for various applications such as nanomachining, plasma diagnose and living cell detection. In the aspect of nanomachining, an X-ray laser offers an alternative to an optical femtosecond laser for generating surface nanostructures because of its shorter attenuation depth, smaller thermal diffusion length [1], and multiple damage mechanisms from thermal and non-thermal processes [2–5]. For many years, research has focused on the interactions of X-ray lasers with various materials. Studies of damage mechanisms and theoretical models continue to explore these interactions.

Si, polymethyl methacrylate (PMMA), amorphous carbon (a-C), and SiO_2, among other materials [6–11], were damaged by femtosecond X-ray lasers at wavelengths of 13.5 nm, 32.5 nm, 86 nm, and 98 nm, respectively. Nanostructures formed on some of the targets [7,9,10]. Reference [7] documents that columnar structures with spacings of several micrometers were found in the ablation areas of Si and SiO_2. The possibility of micromachining insulators with intense ultrashort pulses of extreme ultraviolet radiation were demonstrated. References [9,10] report the detection of laser-induced periodic surface structures (LIPSS) in the ablation areas of a-C and PMMA with spacings of approximately 70 nm, a figure close to the wavelengths of the radiation sources. Interaction experiments typically use nanosecond soft X-ray lasers pumped by capillary discharge and operating at 46.9 nm because of their lower expense, longer gain times, and better stability. In 1999, Rocca et al. [12] first researched the interaction of a 46.9 nm laser focused by a spherical Si/Sc mirror with a multilayer copper coating and obtained damage patterns with diameters of 3 μm. Then Juha et al. [13–18] utilized a 46.9 nm laser to generate nanostructures on PMMA, a-C, and other materials using the same focusing technique. LIPSS was detected in the ablation area with a spacing of several micrometers. The diffraction patterns induced by a mask were observed in the desorption area, where the fluency was greater than zero and less than the threshold. This phenomenon proves a new way to define the threshold of a 46.9 nm laser.

Because the damage mechanism of an optical femtosecond laser is multiphoton absorption, the damage is always induced by more than 1000 laser pulses with a power density higher than 10^{13} W/cm^2. At the same time, most research of femtosecond X-ray lasers does not focus on nanostructure formation. Such lasers are inappropriate for most interaction experiments because of their high cost of operation. In contrast, this paper reports on the cost-effective use of a nanosecond soft X-ray laser for researching nanostructures on a target surface which could be damaged by one single pulse with a power density of 2×10^7 W/cm^2.

* Corresponding author.
E-mail addresses: cuihuaiyu_hit@163.com, 763705458@qq.com (H. Cui).

http://dx.doi.org/10.1016/j.apsusc.2016.11.111
0169-4332/

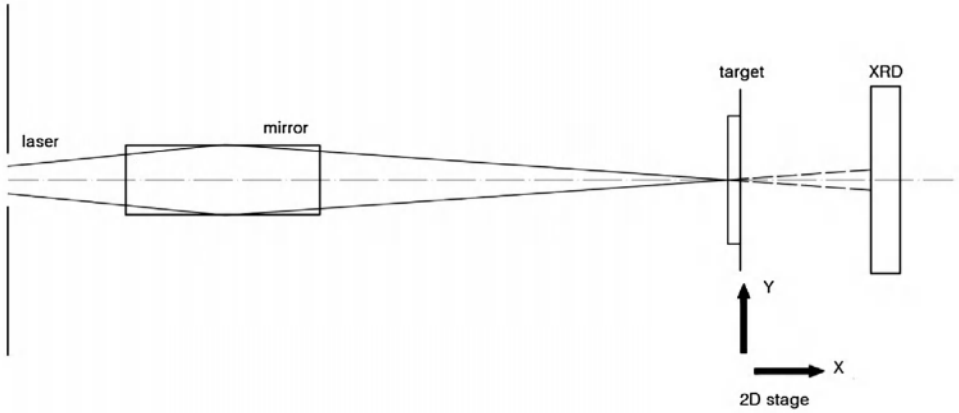

Fig. 1. Outline of the focal beam path.

Dielectric materials with large bandgaps E_g, the energy difference between the bottom conduction band energy and the top valence band energy, are important objects of study as the solid targets in experiments probing the interactions of X-ray lasers with matter [19]. Although these dielectrics are highly transparent to sources of optical radiation up to the vacuum ultraviolet, they are efficiently damaged by X-ray lasers when $h\nu \geq E_g$). In this paper, BaF_2 (E_g = 9.1 eV) was ablated by a capillary-discharge 46.9 nm soft X-ray laser focused by a toroidal mirror at a grazing incidence of 83° and the nanostructures on BaF_2 induced by the laser were studied. This work offers another possibility to dielectrics nanomachining and is useful to research ablation process of X-ray laser. The toroidal mirror, compared with the layer-coated spherical mirrors most often used in soft X-ray laser interaction experiments [12,13], offers reflectivity two times higher. In addition, the laser rarely damages the toroidal mirror because of the grazing incidence [20] and the absence of a coating on the mirror. Further, because of the optical aberration of the mirror, the power density of the focused laser was inhomogeneous; this circumstance could be helpful for conducting research on the variations of damage pattern morphology with different power densities.

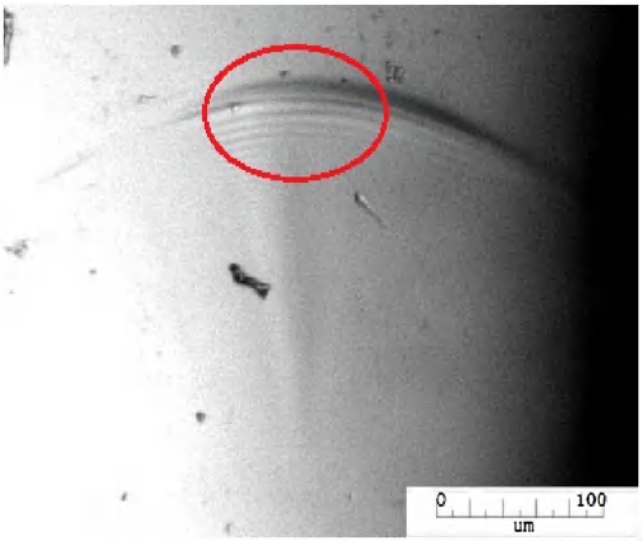

Fig. 2. Optical microscope image of the damaged area induced by 200 pulses of the laser.

2. Material and methods

The 46.9 nm soft X-ray laser operating at 50 μJ used in this experiment was produced using a Ne-like Ar plasma excited with a fast current pulse. The pulse width of the laser was approximately 1.7 ns. Details of the laser are explored elsewhere [21,22]. The general outline of the focal beam path appears in Fig. 1. The toroidal mirror and the X-ray diode (XRD), used to measure the relative energy of the laser, were fixed in place at the bottom of the vacuum chamber. BaF_2, with roughness of less than 5 nm, was used as the target. The target was fastened onto a two-dimensional (2D) stage, positioned perpendicularly to the beam propagation direction. The toroidal mirror focused the laser at a grazing incidence of 83°. The focal length of the mirror was approximately 195 mm. After measurements by the XRD had indicated the output energy of the laser was stable, the target was moved into the beam path by the electric 2D-stage and then irradiated by single or multiple pulses of the soft X-ray laser beam.

The original laser spot at 46.9 nm, when pumped by capillary discharge, exhibited a complex shape because of the instability and asymmetry of the gain medium. Therefore, a YAG:Ce scintillator was used to capture the original and focused laser beam spots. ZEMAX software was used to simulate the focal beam path and to calculate the power density of the spot. Then the shape of the damage induced by the laser could be predicted. Reference [20] describes the details of the real spots and the simulated results.

3. Results and discussion

3.1. Ripple-like structures in the ablation area

Fig. 2 shows the optical microscope image of the damage pattern on BaF_2 induced by 200 pulses of the laser with a power density of $2 \times 10^7 W/cm^2$. The shape of the pattern coincided with the simulations generated by the ZEMAX software. The size of the pattern was approximately 300 μm × 300 μm.

The area encircled with a red ellipse in Fig. 2. was detected by an atomic force microscope (AFM). The results of this imaging appear in Fig. 3. From the three-dimensional (3D) image in Fig. 3(a) we could observe ripple-like structures at the edge line of the damaged area. Then we detected the rest part of the damaged area and these structures were observed all over the damaged area. Fig. 3(b) provides the depth information of the cross section along the black line in Fig. 3(a). Analysis of the structure spacings indicated decreases from 7 μm to 3 μm; the maximum depth of the ripples was approximately 200 nm.

According to Reference [23,24], the capillary discharge laser has an annular profile, which arising from beam refraction along the

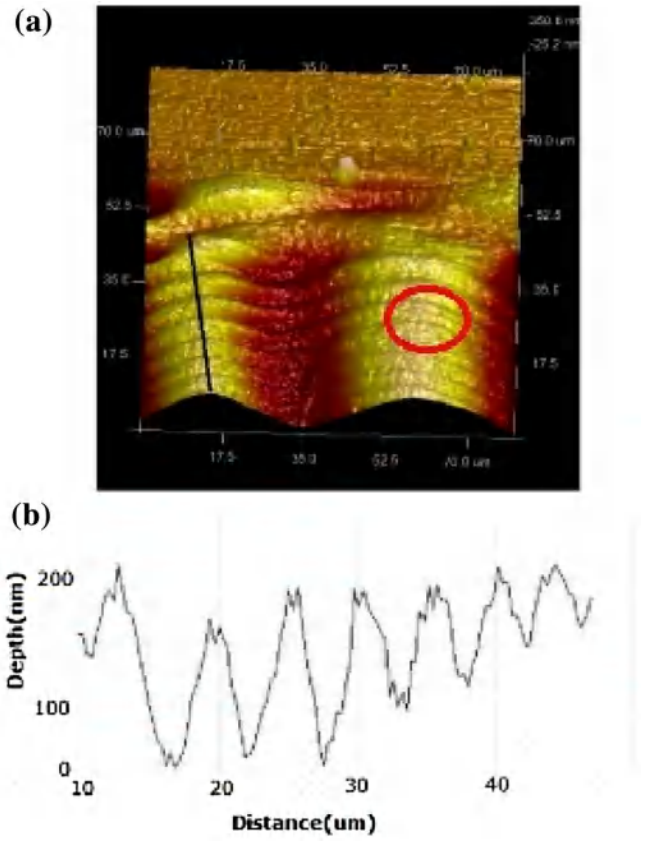

Fig. 3. AFM image of the damage pattern induced by 200 pulses of the laser. (a) 3D image. (b) Depth information of the cross section.

gain medium. Based on the spot image caught by a YAG:Ce scintillator, the shape of capillary discharge 46.9 nm laser used in this experiment is mainly annular profile with several annuluses which are not completely homocentric. We suppose that this asymmetry profile also comes from the beam refraction along the gain medium. And the observed ripples were considered to be induced by the complex energy distribution of the original laser spot. We will do further research on this in the future. We believe that the damage patterns induced by the 46.9 nm laser would be used to analyze the energy distribution of the original laser spot [15].

3.2. Nanostructures in the ablation area

3.2.1. Fringe-like nanostructures in the ablation area

To detect the damage area induced both by a single laser pulse and by 200 laser pulses with a larger amplification, nanostructures covering the area were identified. Fig. 4 shows the AFM 3D images and the cross-section plots of nanostructures detected at the same location on the patterns induced both by the single laser pulse and by 200 laser pulses. The location of Fig. 4(b) was circled with a red ellipse in Fig. 3(a). Both damage areas presented fringe-like structures. The cross-section plots confirmed that the depth of the fringe-like nanostructures induced by single laser pulse was about 10 nm, which was of the order of the attenuation length for BaF_2 at the wavelength of 46.9nm [25,26]. To compare with Fig. 4(a) and (b), the pulse number did not change the spacing of the fringes, which was measured to be approximately 400 nm. In contrast, the morphology of the fringes was changed by the number of laser pulses.

The nanostructure induced by a single laser pulse, as shown in Fig. 4(a), typically presented a valley in the middle of each fringe. We supposed that the laser pulse fractured the BaF_2 surface, introducing microgrooves. The instantaneous absence of the interparticle force resulted in the rise of both sides of each fringe. This process made the middle of each fringe lower than its sides, thus forming the valley. There is still no explicit theory that accounts for the formation of the fringes induced by a 46.9 nm laser on a BaF_2 surface. However, in our other related experiments, until now, the same fringe-like patterns were not observed in the surfaces of SiO_2, Cu, and Si. Fig. 5 shows the AFM images of the ablation area in Si, Cu and SiO_2. In Fig. 5(b), the melting surface was observed, which was mentioned in Referene [20]. And in Fig. 5(a) and (c), no clear nanostructures were observed. These three images show the

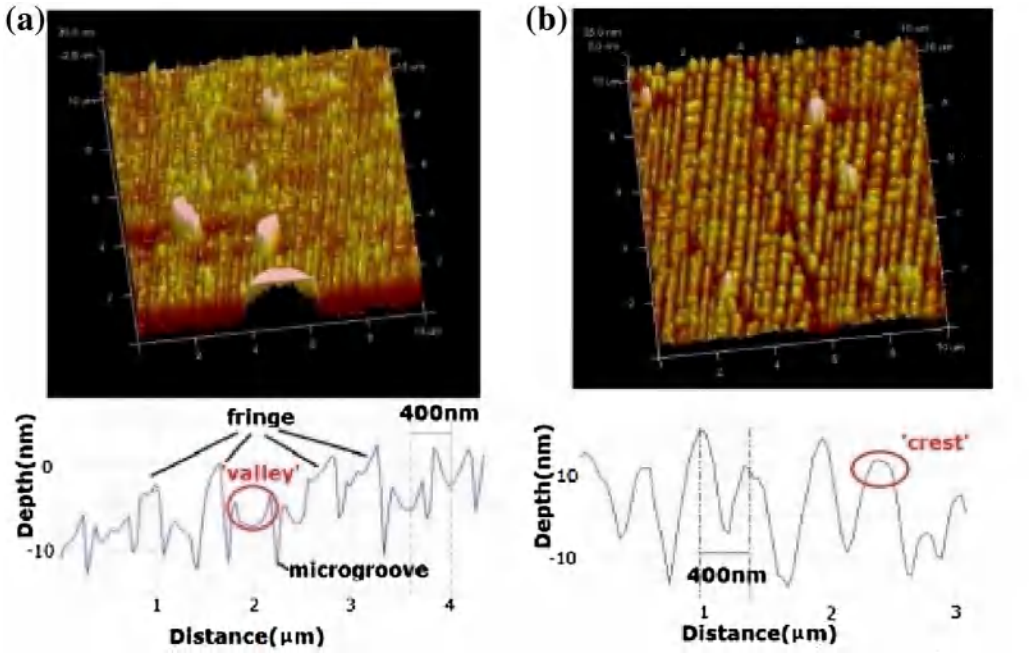

Fig. 4. Nanostructures on BaF_2 surface induced by (a) one pulse and (b) 200 pulses of the laser.

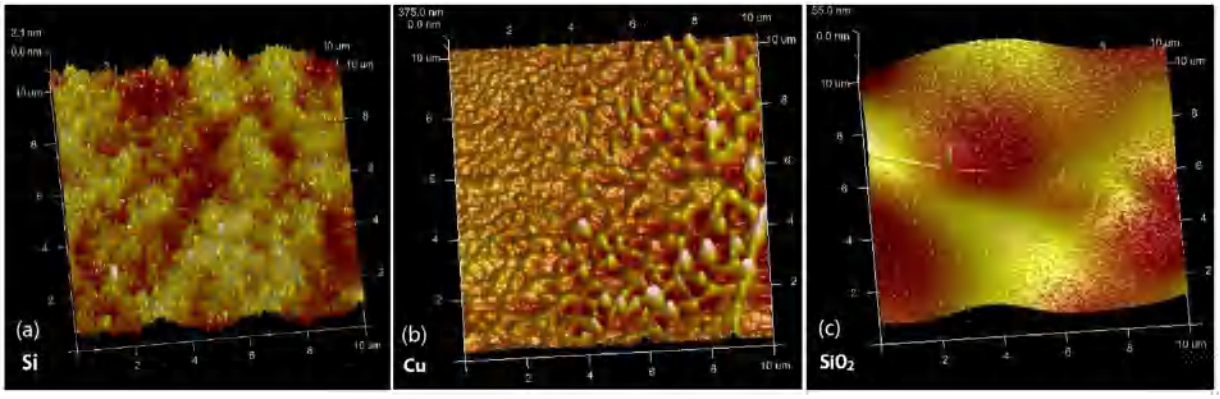

Fig. 5. AFM images of ablation area in Si, Cu and SiO_2.

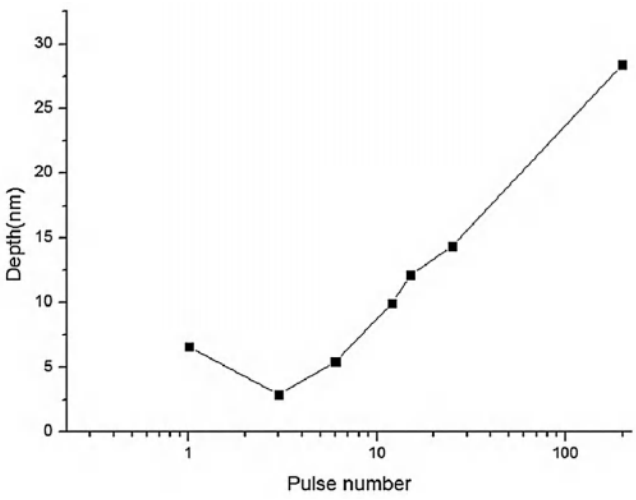

Fig. 6. Variation of the depth of the fringes with the laser pulse number.

evidence that there are no same fringe-like nanostructures as observed in BaF_2 formed in the ablation area of Si, Cu and SiO_2.

By referring to work by Varlamova [27], we hypothesized a model for the interaction process. Two processes occurred during the interaction of multiple laser pulses with the BaF_2. In the first process, after the damage from the first laser pulse, the fringes on the BaF_2 surface would result in the inhomogeneous energy absorption of the following laser pulses. The material density of the microgroove would be higher than the material density of the area on the fringes. Therefore, in response to being targeted by the laser in the same proportions, more particles in the microgrooves would absorb the energy of the laser photons and then be ejected. Thus, the microgrooves would grow deeper. In contrast, in the second process, particle self-diffusion tended to smooth the surface by filling the microgrooves with diffused particles from the fringes. Then the valley changed into a crest, as shown in Fig. 4(b).

Fig. 6 shows the variation of the fringe depths from 3 nm to 30 nm with the laser pulse numbers of 1, 3, 6, and up to 200. Except in the case of a single pulse, the depth of the fringes increased with the increase in the laser pulse number. However, because of the second process mentioned above, the two parameters did not show a linear relationship. According to the analysis depicted in Fig. 6. we supposed that in the first several laser pulses (one to six pulses), the second process formed the leading cause of the damage because of the distinct valley-like structures induced by the first laser pulse. Then the first process played a dominant role. The following laser

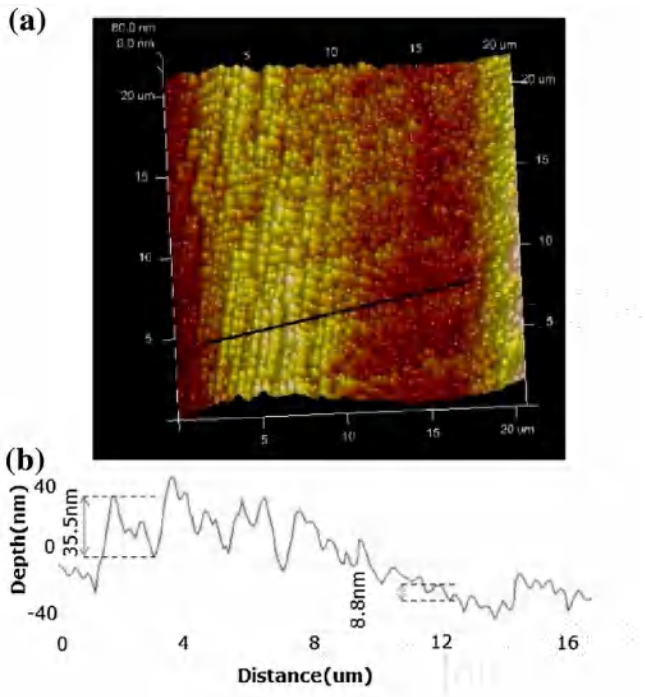

Fig. 7. Different morphology of the damaged area induced by the X-ray laser at different power densities. (a) 3D AFM image. (b) Depth information of the cross section.

pulses (6 to 200 pulses) deepened the microgrooves. Afterward, the second process again dominated and smoothed the surface in response to surface tension. Therefore, the information in Fig. 6. provides evidence of the two processes in competition.

3.2.2. Mastoid nanostructures in the ablation area

The fringe-like structures were detected covering the whole damaged area. And at certain locations they presented to be mastoid-like shape shown in Fig. 7(a). The nanostructures were induced by 200 laser pulses. Fig. 7(b) presents the depth information of the cross section along the black line in Fig. 7(a). Mastoid structures appeared with diameters of approximately 600 nm. About the formation of mastoid structures, we made the speculation. First fringe-like structures were formed by the effect of first several laser pulses. Then fringes broke into pieces in certain ablation environment. After that, due to the effect of the following laser pulses, the broke surface was smoothed by the effect of particle self-diffusion and the fringe-like structures changed into mastoids. We

gave this conjecture because the mastoids structures only appeared in several locations of the damaged area induced by multiple laser pulses.

According to the overall trend of the morphology, the red area, which was deeper than the yellow area in Fig. 7(a), was induced by part of the focused laser spot at higher power densities. By analyzing the information in Fig. 7(b), the height of one selected mastoid in the red area was measured to be 8.8 nm; in the yellow area, the height was measured to be 35.5 nm. Most of the mastoids in the yellow area were three to four times higher than those in the red area. We attributed this phenomenon to the effects of asymmetrical power density of the focused laser spot. An explanation resting on the second process mentioned above suggests that more particles located at the top of the mastoid would fill in the microgrooves because of the laser focusing with a higher power density. Therefore, the mastoid grew shorter. In contrast, the mastoid induced by the laser at a lower power density would be higher. This phenomenon helped with performing damage mechanism analysis. More research is needed to confirm the statement relating these processes to the formation of the nanostructure morphology.

4. Conclusion

The experiment presented in this paper produced new nanostructures, induced by a capillary-discharge 46.9 nm soft X-ray laser, on a BaF_2 surface. The laser pulse number was varied from 1 pulse to 200 pulses. Fringe-like nanostructures with the spacing of approximately 400 nm and mastoid nanostructures with the diameter of approximately 600 nm were researched. An analysis of the causes of the depths of nanostructures indicated they were influenced by variations in the pulse number and power density of the laser. In cases of multiple-laser pulse damage, the model explained that nanostructures were induced by the competition of two processes: surface damage from particle emission and smoothing from particle self-diffusion.

Funding

This work was supported by the National Natural Foundation of China (No. 61275139).

References

[1] G. Norman, S. Starikov, V. Stegailov, V. Fortov, I. Skobelev, T. Pikuz, A. Faenov, S. Tamotsu, Y. Kato, M. Ishino, M. Tanaka, N. Hasegawa, M. Nishikino, T. Ohba, T. Kaihori, Y. Ochi, T. Imazono, Y. Fukuda, M. Kando, T. Kawachi, Nanomodification of gold surface by picosecond soft x-ray laser pulse, J. Appl. Phys. 112 (2012), http://dx.doi.org/10.1063/1.4731752.

[2] M. Grisham, G. Vaschenko, C.S. Menoni, J.J. Rocca, Y.P. Pershyn, E.N. Zubarev, D.L. Voronov, V. a Sevryukova, V.V. Kondratenko, a V Vinogradov, I. a Artioukov, Damage to extreme-ultraviolet Sc/Si multilayer mirrors exposed to intense 46.9-nm laser pulses, Opt. Lett. 29 (2004) 620–622 http://www.ncbi.nlm.nih.gov/pubmed/15035490.

[3] J. Chalupský, L. Juha, V. Hájková, J. Cihelka, L. Vysín, J. Gautier, J. Hajdu, S.P. Hau-Riege, M. Jurek, J. Krzywinski, R. a London, E. Papalazarou, J.B. Pelka, G. Pelka, S. Sebban, R. Sobierajski, N. Stojanovic, K. Tiedtke, S. Toleikis, T. Tschentscher, C. Valentin, H. Wabnitz, P. Zeitoun, Non-thermal desorption/ablation of molecular solids induced by ultra-short soft x-ray pulses, Opt. Express 17 (2009) 208–217, http://dx.doi.org/10.1364/OE.17.000208.

[4] N.A. Inogamov, A.Y. Faenov, V.A. Khokhlov, V.V. Zhakhovskii, Y.V. Petrov, I.Y. Skobelev, K. Nishihara, Y. Kato, M. Tanaka, T.A. Pikuz, M. Kishimoto, M. Ishino, M. Nishikino, Y. Fukuda, S.V. Bulanov, T. Kawachi, S.I. Anisimov, V.E. Fortov, Spallative ablation of metals and dielectrics, Contrib. Plasma Phys. 49 (2009) 455–466, http://dx.doi.org/10.1002/ctpp.200910045.

[5] N.A. Inogamov, V.V. Zhakhovsky, A.Y. Faenov, V.A. Khokhlov, V.V. Shepelev, I.Y. Skobelev, Y. Kato, M. Tanaka, T.A. Pikuz, M. Kishimoto, M. Ishino, M. Nishikino, Y. Fukuda, S.V. Bulanov, T. Kawachi, Y.V. Petrov, S.I. Anisimov, V.E. Fortov, Spallative ablation of dielectrics by X-ray laser, Appl. Phys. A Mater. Sci. Process. 101 (2010) 87–96, http://dx.doi.org/10.1007/s00339-010-5764-3.

[6] N. Stojanovic, D. Von Der Linde, K. Sokolowski-Tinten, U. Zastrau, F. Perner, E. Forster, R. Sobierajski, R. Nietubyc, M. Jurek, D. Klinger, J. Pelka, J. Krzywinski, L. Juha, J. Cihelka, A. Velyhan, S. Koptyaev, V. Hajkova, J. Chalupsky, J. Kuba, T. Tschentscher, S. Toleikis, S. Dusterer, H. Redlin, Ablation of solids using a femtosecond extreme ultraviolet free electron laser, Appl. Phys. Lett. 89 (2006) 89–91, http://dx.doi.org/10.1063/1.2405398.

[7] J. Krzywinski, R. Sobierajski, M. Jurek, R. Nietubyc, J.B. Pelka, L. Juha, M. Bittner, V. Ĺtal, V. Vorlíček, A. Andrejczuk, J. Feldhaus, B. Keitel, E.L. Saldin, E.A. Schneidmiller, R. Treusch, M.V. Yurkov, Conductors, semiconductors, and insulators irradiated with short-wavelength free-electron laser, J. Appl. Phys. 101 (2007) 2–5, http://dx.doi.org/10.1063/1.2434989.

[8] J. Andreasson, B. Iwan, A. Andrejczuk, E. Abreu, M. Bergh, C. Caleman, A.J. Nelson, S. Bajt, J. Chalupsky, H.N. Chapman, R.R. Fäustlin, V. Hajkova, P.A. Heimann, B. Hjörvarsson, L. Juha, D. Klinger, J. Krzywinski, B. Nagler, G.K. Pálsson, W. Singer, M.M. Seibert, R. Sobierajski, S. Toleikis, T. Tschentscher, S.M. Vinko, R.W. Lee, J. Hajdu, N. Tîmneanu, Saturated ablation in metal hydrides and acceleration of protons and deuterons to keV energies with a soft-x-ray laser, Phys. Rev. E – Stat. Nonlinear Soft Matter Phys. 83 (2011) 1–7, http://dx.doi.org/10.1103/PhysRevE.83.016403.

[9] B. Steeg, L. Juha, J. Feldhaus, S. Jacobi, R. Sobierajski, C. Michaelsen, A. Andrejczuk, J. Krzywinski, Total reflection amorphous carbon mirrors for vacuum ultraviolet free electron lasers, Appl. Phys. Lett. 84 (2004) 657–659, http://dx.doi.org/10.1063/1.1645320.

[10] L. Juha, Short-wavelength ablation of molecular solids: pulse duration and wavelength effects, J. Micro/Nanolithogr. MEMS MOEMS 4 (2005) 033007, http://dx.doi.org/10.1117/1.2037467.

[11] S.P. Hau-Riege, H.N. Chapman, J. Krzywinski, R. Sobierajski, S. Bajt, R.A. London, M. Bergh, C. Caleman, R. Nietubyc, L. Juha, J. Kuba, E. Spiller, S. Baker, R. Bionta, K. Sokolowski Tinten, N. Stojanovic, B. Kjornrattanawanich, E. Gullikson, E. Plonjes, S. Toleikis, T. Tschentscher, Subnanometer-scale measurements of the interaction of ultrafast soft X-ray free-electron-laser pulses with matter, Phys. Rev. Lett. 98 (2007) 1–4, http://dx.doi.org/10.1103/PhysRevLett.98.145502.

[12] B.R. Benware, A. Ozols, J.J. Rocca, I. a Artioukov, V.V. Kondratenko, a V. Vinogradov, Focusing of a tabletop soft-x-ray laser beam and laser ablation, Opt. Lett. 24 (1999) 1714–1716, http://dx.doi.org/10.1364/OL.24.001714.

[13] L. Juha, M. Bittner, D. Chvostova, J. Krasa, Z. Otcenasek, A.R. Präg, J. Ullschmied, Z. Pientka, J. Krzywinski, J.B. Pelka, A. Wawro, M.E. Grisham, G. Vaschenko, C.S. Menoni, J.J. Rocca, Ablation of organic polymers by 46.9-nm-laser radiation, Appl. Phys. Lett. 86 (2005) 1–3, http://dx.doi.org/10.1063/1.1854741.

[14] L. Juha, V. Hájková, J. Chalupsk, V. Vorlíček, A. Ritucci, A. Reale, P. Zuppella, M. Störmer, Radiation damage to amorphous carbon thin films irradiated by multiple 46.9 nm laser shots below the single-shot damage threshold, J. Appl. Phys. 105 (2009), http://dx.doi.org/10.1063/1.3117515.

[15] L. Vyšín, T., Burian, J. Chalupský, M. Grisham, V. Hájková, S. Heinbuch, K., Jakubczak, D., Martz, T., Mocek, P., Pira, J., Polan, J.J., Rocca, B., Rus, J., Sobota, L. Juha, Characterization of the focused beam from a 10-Hz desktop capillary-discharge 46. 9-nm laser, 7361 (n.d.) 1–8. 10.1117/12.822759.

[16] K. Kolacek, J. Straus, J. Schmidt, O. Frolov, V. Prukner, A. Shukurov, V. Holy, J. Sobota, T. Fort, Nano-structuring of solid surface by extreme ultraviolet Ar8+ laser, Laser Part. Beams 30 (2011) 57–63, http://dx.doi.org/10.1017/S0263034611000681.

[17] O. Frolov, K. Kolacek, J. Straus, J. Schmidt, V. Prukner, A. Shukurov, Generation and application of the soft X-ray laser beam based on capillary discharge, J. Phys. Conf. Ser. 511 (2014) 012035, http://dx.doi.org/10.1088/1742-6596/511/1/012035.

[18] K. Kolacek, J. Schmidt, Interaction of extreme ultraviolet laser radiation with solid surface: ablation, desorption, nanostructuring, High Power 9255 (2015) 25–29 (92553u\r10.1117/12.2071273).

[19] A. Ritucci, G. Tomassetti, A. Reale, L. Arrizza, L. Reale, L. Palladino, F. Flora, F. Bonfigli, T. Pikuz, J. Kaiser, J. Nilsen, A.F. Jankowski, Damage and ablation of large band gap dielectrics induced by a 46. 9 nm laser beam, Opt. Lett. (2006).

[20] Y. Zhao, H. Cui, W. Zhang, W. Li, S. Jiang, L. Li, Si and Cu ablation with a 469-nm laser focused by a toroidal mirror, Opt. Express 23 (2015) 14126, http://dx.doi.org/10.1364/oe.23.014126.

[21] Y. Zhao, M. Mo, Y. Xie, S. Yang, Q. Wang, Observation of a saturated soft X-ray laser in a low current capillary discharge, in: Conference on Lasers and Electro-Optics/Pacific Rim, Optical Society of America, 2009, WD2_4.

[22] Y. Zhao, S. Jiang, Y. Xie, D. Yang, S. Teng, D. Chen, Q. Wang, Demonstration of soft x-ray laser of Ne-like Ar at 69.8 nm pumped by capillary discharge, Opt. Lett. 36 (2011) 3458–3460, http://dx.doi.org/10.1364/OL.36.003458.

[23] Juan L.A. Chilla, Jorge J. Rocca, Beam optics of gain-guided soft-x-ray lasers in cylindrical plasmas, J. Opt. Soc. Am. B 13 (1996) 2841–2852, http://dx.doi.org/10.1364/JOSAB.13.002841.

[24] V. Aslanyan, I. Kuznetsov, H. Bravo, M.R. Woolston, A.K. Rossall, C.S. Menoni, J.J. Rocca, G.J. Tallents, Ablation and transmission of thin solid targets irradiated by intense extreme ultraviolet laser radiation, APL Photonics 1 (2016) 066101.

[25] B.L. Henke, E.M. Gullikson, J.C. Davis, X-ray interactions: photoabsorption, scattering, transmission, and reflection at E = 50–30000 eV, Z = 1–92, At. Data Nucl. Data Tables 54 (1993) 181–342.

[26] C.T. Chantler, Theoretical form factor attenuation, and scattering tabulation for Z = 1–92 from E = (1–10 eV) to (0. 4–1.0 MeV), J. Phys. Chem. Ref. Data 24 (1995) 71–643.

[27] O. Varlamova, F. Costache, J. Reif, M. Bestehorn, Self-organized pattern formation upon femtosecond laser ablation by circularly polarized light, Appl. Surf. Sci. 252 (2006) 4702–4706, http://dx.doi.org/10.1016/j.apsusc.2005.08.120.